Order in Phospholipid Langmuir-Blodgett Monolayers Determined by Total Internal Reflection Fluorescence

Xin Zhai and J. Mieke Kleijn*
Department of Physical and Colloid Chemistry, Wageningen Agricultural University, Dreijenplein 6, 6703 HB Wageningen, The Netherlands

ABSTRACT Orientational order parameters of two diphenylhexatriene (DPH)-based fluorescent probes, 2-(3-(diphenylhexatrienyl)propanoyl)-1-hexadecanoyl-sn-glycero-3-phosphocholine (DPHpPC) and 1-(4-trimethylammoniumphenyl)-6-phenyl-1,3,5-hexatriene (TMA-DPH), in dipalmitoylphosphatidylcholine (DPPC) Langmuir-Blodgett monolayers on quartz have been determined by total internal reflection fluorescence (TIRF). From these order parameters orientation distributions were reconstructed by the maximum-entropy method. For monolayers transferred from the liquid-condensed phase, preferential tilt angles with respect to the substrate normal around 14° in the tail region and 5° near the glycerol-acyl chain linkage were found, as reflected by the DPHpPC and TMA-DPH probes, respectively. The degree of ordering near the headgroup region seems to be larger than that further away from the surface. A substantial fraction of the TMA-DPH probes have a flat orientation and are probably located between the phospholipid headgroups and the substrate surface. Monolayers transferred from the liquid-expanded phase show a more random ordering, and most of the probe molecules (DPHpPC) are more or less flat on the surface. The results are consistent with earlier atomic force microscopy measurements on identical monolayers and are in reasonable agreement with previously published data on other organized phospholipid systems.

INTRODUCTION

Biological membranes are dynamic structures in which the molecular orientational order is generally believed to play an essential role in the maintenance of membrane functions. Apart from its significance for other membrane properties such as lipid-bound protein mobility, molecular organization is a crucial factor in membrane permeability. This is illustrated, for example, by the finding that the permeability of one-component phospholipid bilayers to small water-soluble molecules exhibits a maximum in the coexistence region of gel and fluid domains (Clerc and Thompson, 1995). It has been shown that for phospholipid monolayers adsorbed on a mercury electrode surface, the permeability for metal ions dramatically depends on the applied electrical potential (Nelson and van Leeuwen, 1989). Using a theoretical model for the phospholipid monolayer, it was demonstrated that this potential-dependent behavior can be explained in terms of structural variations (Leermakers and Nelson, 1990).

Phospholipid films on solid supports are attracting increasing attention as model systems for biological membranes, as well as for their application in biosensor devices (Sharma and Rogers, 1994; Nikolelis et al., 1995). The significance of such model systems is suggested by, e.g., theoretical models and numerical simulations which show that the segment density profile for a lipid monolayer on a solid substrate resembles half the profile of a lamellar bilayer membrane (Leermakers and Nelson, 1990; Hasmonay et al., 1994). It has been found experimentally that electron diffraction patterns obtained from supported phospholipid monolayers appear to be the same as those obtained from free-standing bilayers (Hui et al., 1974).

It is our intention to investigate the relationship between the molecular organization and ion permeability in phospholipid mono- and bilayers on solid substrates. One of the experimental techniques involved is total internal reflection fluorescence (TIRF), by which it is possible to determine the orientation distribution of fluorophores in an adsorption layer on optically transparent substrates (Thompson and Burghardt, 1986; Bos and Kleijn, 1995a,b). By using optically transparent conductive films deposited on quartz slides as the substrates, TIRF can be combined with electrochemical techniques. This allows simultaneous determination of the order in phospholipid layers and their permeability for metal ions and other (electroactive) compounds.

In this paper we present the first results of TIRF orientation measurements on dipalmitoylphosphatidylcholine (DPPC) monolayers transferred on quartz by the Langmuir-Blodgett (LB) technique, using the fluorescent probes 2-(3-(diphenylhexatrienyl)propanoyl)-1-hexadecanoyl-sn-glycero-3-phosphocholine (DPHpPC) and 1-(4-trimethyammoniumphenyl)-6-phenyl-1,3,5-hexatriene (TMA-DPH). To our knowledge, this is the first time that the order in single phospholipid monolayers on solid substrates has been measured. Diphenylhexatriene (DPH) and its derivates are commonly used for the determination of orientational order and dynamics in biomembrane studies. The DPHpPC molecule is a phospholipid with the DPH moiety covalently attached to the *sn*-2 position in one of the lipid chains (see Fig. 1), and therefore it provides structural information on

Received for publication 25 October 1996 and in final form 24 February 1997.

Address reprint requests to Dr. J. Mieke Kleijn, Department of Physical and Colloid Chemistry, Agricultural University, P.O. Box 8038, 6700 EK Wagenigen, The Netherlands. Tel.: 31-317-482145/482178; Fax: 31-317-483777; E-mail: mieke@fenk.wau.nl.

0006-3495/97/06/2651/09 $2.00

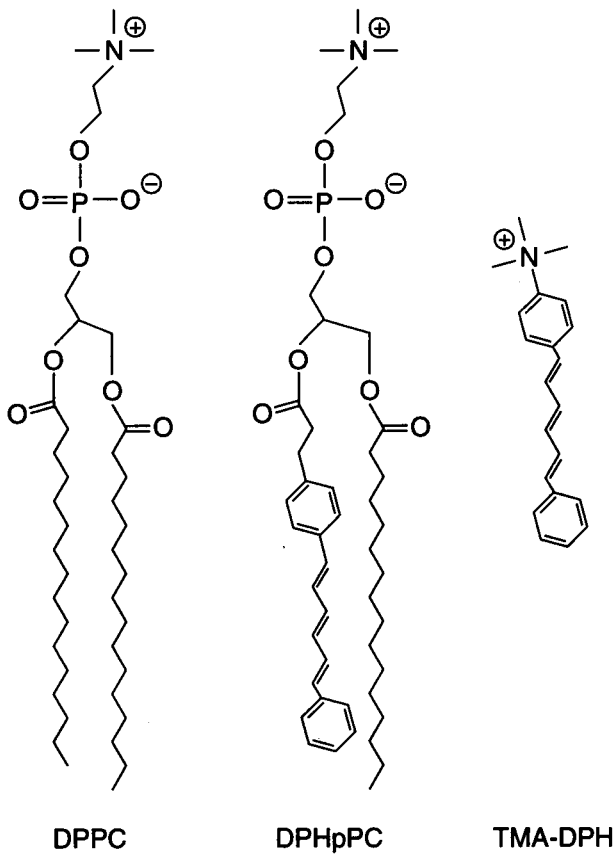

FIGURE 1 Structure formulas of the fluorescence probes DPHpPC and TMA-DPH and their locations in a DPPC bilayer.

the lipid chain order. TMA-DPH is expected to be anchored with its charged group in the headgroup region of phospholipid mono- and bilayers, and therefore reflects molecular order near the glycerol-acyl chain linkage (Parente and Lentz, 1985; Lentz, 1989). First we derive expressions to obtain the second- and fourth-rank order parameters $\langle P_2 \rangle$ and $\langle P_4 \rangle$ of the orientation distributions of the probes from TIRF measurements. Orientation distributions are calculated from $\langle P_2 \rangle$ and $\langle P_4 \rangle$ using the maximum-entropy method. Besides the orientation of the probes, the angle between their absorption and emission dipole moments is also evaluated.

THEORY

The theory underlying orientation measurements using TIRF has been described before in general terms (Bos and Kleijn, 1995a). Here we treat the case where the fluorophore is a cylindrically symmetrical moiety, in which the absorption dipole moment is parallel with the long molecular axis, as is the case for DPH-based probes (Kooyman et al., 1983; Lentz, 1989). The direction of the emission dipole moment of DPH and its derivates is less well defined and has been reported to depend on the molecular environment (Kooyman et al., 1983; Van Ginkel et al., 1986; Van Langen et al., 1987; Deinum et al., 1988). Kooyman et al. (1983) and Lentz (1989) have discussed this phenomenon and explained it as being caused by the coupling of two excited states.

In TIRF, fluorescent molecules at or near an optically transparent solid interface are selectively excited by an evanescent wave, created by the total internal reflection of a laser beam at this interface. By variation of the polarization angle Ψ of the incident light beam, the direction of the electric field component of the evanescent field is changed. As a result, the interaction between the transition dipole moments of the fluorophores and the evanescent field is modified, which, in turn, gives rise to a change in the fluorescence signal. It has been shown (Bos and Kleijn, 1995a) that by measuring both the fluorescence intensity and its polarization as a function of the polarization angle of the incident light, all of the principal information available on the orientation distribution of the fluorophores enclosed in the fluorescence signal (i.e., the order parameters $\langle P_2 \rangle$ and $\langle P_4 \rangle$) can be retrieved.

Assuming that the orientation of the molecules does not change significantly on the time scale of fluorescence and that energy transfer between the fluorophores is negligible, the parallel and perpendicular polarized components of the detected fluorescence are given by

$$F_{\parallel} = C\langle(\boldsymbol{\mu} \cdot \mathbf{E})^2 f_{\parallel}(\boldsymbol{\nu})\rangle \tag{1a}$$

$$F_{\perp} = C\langle(\boldsymbol{\mu} \cdot \mathbf{E})^2 f_{\perp}(\boldsymbol{\nu})\rangle \tag{1b}$$

where the vectors $\boldsymbol{\mu}$ and $\boldsymbol{\nu}$ stand for the directions of the absorption and emission transition dipole moments of the excited molecule, respectively; $\mathbf{E}$ represents the direction of the electric field vector of the evanescent field; and $f_{\parallel}(\boldsymbol{\nu})$ and $f_{\perp}(\boldsymbol{\nu})$ are the collection efficiencies for the parallel and perpendicular components of the fluorescence, respectively. The constant C incorporates the magnitude of the absorption and emission dipole moments, the quantum yield, and experimental parameters such as the surface concentration of fluorophores, the intensity of the evanescent field, and properties of the detection system. The angle brackets $\langle\ \rangle$ in Eq. 1 denote a time and ensemble average over all abundant orientations of the fluorescent groups in the sample.

Both assumptions made to arrive at Eq. 1 seem to be reasonable for the systems studied here. It can be shown that in the limiting case of large rotational movements with correlation times much smaller than the fluorescence lifetime, polarization of the fluorescence is completely lost, and only the second-rank order parameter $\langle P_2 \rangle$ can be retrieved. This is not the case here. In the fluorescence time region, the only mode that gives rise to fluorescence depolarization is rotational diffusion along directions perpendicular to the long symmetry axis of the DPH moiety, usually described for lipid bilayers as wobbling motion (Cheng, 1989). Literature values for the rotation correlation times for DPHpPC and TMA-DPH in gel-phase lipid bilayers, as determined from time-resolved fluorescence anisotropy measurements, vary between 1 and 8 ns (Mulders et al., 1986; Cheng, 1989;

Muller et al., 1994a,b; Bernsdorff et al., 1995), whereas the fluorescence lifetimes of these probes are in exactly the same range (Parente and Lentz, 1985; Van Ginkel et al., 1986; Cheng, 1989; Lentz, 1989; Bernsdorff et al., 1995). In the gel phase wobbling motions are fairly restricted, with maximum deviations of 10–20° from the mean orientation angle (Parente and Lentz, 1985; Lentz, 1989; Florine-Casteel, 1990). It is to be expected that for phospholipid monolayers on solid substrates the rotational diffusion is even more restricted. Because the absorption and emission spectra of DPH probes show very little overlap (Shinitzky and Barenholz, 1974; Lentz, 1989), energy transfer between the probes, which would cause fluorescence depolarization, is negligible.

Defining an orthogonal coordinate system in which the xy plane corresponds to the interface and the xz plane to the plane of incidence, the direction of $\mathbf{E}$ can be given in terms of the relative magnitudes of its x, y, and z components. These vary with the polarization of the incident light beam in the following way (Harrick, 1967):

$$E_x = \epsilon_x \cos \Psi \tag{2a}$$

$$E_y = \epsilon_y \sin \Psi \tag{2b}$$

$$E_z = \epsilon_z \cos \Psi \tag{2c}$$

The values of ϵ_x, ϵ_y, and ϵ_z depend on the refractive indices of the media at both sides of the interface and on the angle of incidence, as described by Harrick (1967).

For a pulsed excitation of the fluorophores and detection along the normal of the interface, here defined as the z axis, the collection efficiencies of the two polarized components of the fluorescence are given by (Axelrod, 1979)

$$f_{\parallel}(\boldsymbol{\nu}) = \nu_x^2 + \tfrac{1}{2}(1 - \gamma)\nu_z^2 \tag{3a}$$

$$f_{\perp}(\boldsymbol{\nu}) = \nu_y^2 + \tfrac{1}{2}(1 - \gamma)\nu_z^2 \tag{3b}$$

where γ is the dichroic factor, depending on the aperture angle of the detection system (Burghardt and Thompson, 1984).

The direction of the absorption dipole moment $\boldsymbol{\mu}$ of the fluorescent group in the xyz coordinate system is described by a polar angle θ and an azimuthal angle ϕ, as depicted in Fig. 2. To describe the direction of the emission dipole moment $\boldsymbol{\nu}$, we define a second coordinate system $x'y'z'$ in which the z' axis is parallel to the absorption dipole moment. In this coordinate system the direction of $\boldsymbol{\nu}$ is given by a polar angle β (i.e., the angle between the absorption and emission dipole moments) and an azimuthal angle α (see Fig. 2). The expressions for the two vectors $\boldsymbol{\mu}$ and $\boldsymbol{\nu}$ in the xyz coordinate system are

$$\boldsymbol{\mu} = \begin{pmatrix} \cos\phi \sin\theta \\ \sin\phi \sin\theta \\ \cos\theta \end{pmatrix} \tag{4a}$$

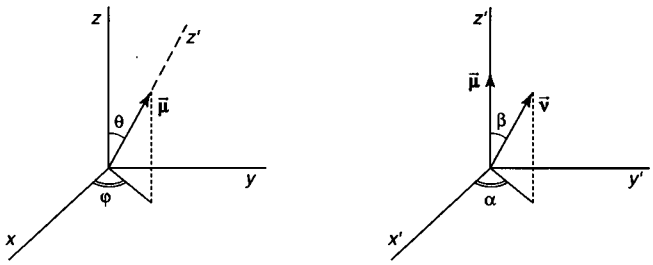

FIGURE 2 Definition of the orientation angles of the transition dipole moments of the DPH group. On the left is the laboratory frame, in which the xy plane corresponds to the substrate surface. The direction of the absorption dipole moment, $\boldsymbol{\mu}$, is given by angles ϕ and θ. On the right is the molecular frame, in which the z' axis represents the long molecular axis of DPH ($\boldsymbol{\mu}$ is parallel to this axis). In this coordinate system the direction of the emission dipole moment, $\boldsymbol{\nu}$, is defined by angles α and β.

$$\boldsymbol{\nu} = \begin{pmatrix} \cos\phi\cos\theta\cos\alpha\sin\beta - \sin\phi\sin\alpha\sin\beta \\ \qquad + \cos\phi\sin\theta\cos\beta \\ \sin\phi\cos\theta\cos\alpha\sin\beta + \cos\phi\sin\alpha\sin\beta \\ \qquad + \sin\phi\sin\theta\cos\beta \\ -\sin\theta\cos\alpha\sin\beta + \cos\theta\cos\beta \end{pmatrix} \tag{4b}$$

By using Eqs. 3 and 4, Eq. 1 can be elaborated into expressions for $F_{\parallel}$ and $F_{\perp}$ in terms of the orientation angles of the transition dipole moments, α, β, ϕ, and θ. These expressions can be simplified by assuming that the interface is isotropic in the x and y directions, so that all values for ϕ and α have the same probability. This assumption seems to be justified for the substrate used here: there is no preferential direction on the quartz surface. Therefore, the angles ϕ and α can be eliminated from the expressions for $F_{\parallel}$ and $F_{\perp}$ by integration over α and ϕ from 0 to 2π. Furthermore, the angle β between the absorption and emission dipole moments is taken as a constant, i.e., in a particular phospholipid monolayer β is assumed to be the same for all DPH probe molecules. Thus the orientation distribution of the molecules is given by a normalized orientation distribution function in θ only, $N(\theta)$, and the expressions for the fluorescence intensities $F_{\parallel}$ and $F_{\perp}$ become

$$\begin{aligned} F_{\parallel} = \frac{1}{16}C\{&(3 - 2\gamma)E_x^2 + (5 - 2\gamma)E_y^2 \\ &+ \langle\cos^2\theta\rangle[(-2 + 4\gamma)E_x^2 + (-6 + 4\gamma)E_y^2 + (8 - 4\gamma)E_z^2] \\ &+ \langle\cos^4\theta\rangle[(-1 - 2\gamma)E_x^2 + (1 - 2\gamma)E_y^2 + 4\gamma E_z^2] \\ &+ \cos^2\beta[(3 + 2\gamma)E_x^2 + (-3 + 2\gamma)E_y^2] \\ &+ \langle\cos^2\theta\rangle\cos^2\beta[(-6 - 8\gamma)E_x^2 + (6 - 8\gamma)E_y^2 + 4\gamma E_z^2] \\ &+ \langle\cos^4\theta\rangle\cos^2\beta[(3 + 6\gamma)E_x^2 + (-3 + 6\gamma)E_y^2 - 12\gamma E_z^2]\} \end{aligned} \tag{5a}$$

$$\begin{aligned} F_{\perp} = \frac{1}{16}C\{&(5 - 2\gamma)E_x^2 + (3 - 2\gamma)E_y^2 \\ &+ \langle\cos^2\theta\rangle[(-6 + 4\gamma)E_x^2 + (-2 + 4\gamma)E_y^2 + (8 - 4\gamma)E_z^2] \\ &+ \langle\cos^4\theta\rangle[(1 - 2\gamma)E_x^2 + (-1 - 2\gamma)E_y^2 + 4\gamma E_z^2] \\ &+ \cos^2\beta[(-3 + 2\gamma)E_x^2 + (3 + 2\gamma)E_y^2] \\ &+ \langle\cos^2\theta\rangle\cos^2\beta[(6 - 8\gamma)E_x^2 + (-6 - 8\gamma)E_y^2 + 4\gamma E_z^2] \\ &+ \langle\cos^4\theta\rangle\cos^2\beta[(-3 + 6\gamma)E_x^2 + (3 + 6\gamma)E_y^2 - 12\gamma E_z^2]\} \end{aligned} \tag{5b}$$

in which

$$\langle x \rangle \equiv \int_{\theta=0}^{\pi} x\, N(\theta) \sin\theta \, d\theta \tag{6}$$

By using Eq. 2 it can be shown that the fluorescence intensities depend on the polarization angle Ψ of the incident light as

$$F_{\parallel}(\Psi) = C(A_{\parallel} + B_{\parallel}\cos^2\Psi) \tag{7a}$$

$$F_{\perp}(\Psi) = C(A_{\perp} + B_{\perp}\cos^2\Psi) \tag{7a}$$

in which $A_{\parallel}$, $B_{\parallel}$, $A_{\perp}$, and $B_{\perp}$ are functions of the orientation distribution of the fluorophores, the dichroic factor γ, and ϵ_x, ϵ_y, and ϵ_z. From Eq. 7 it follows that four measurements suffice to disclose all available information concerning the orientation distribution as reflected in the fluorescence response of the system. The constant C, two θ-related parameters ($\langle\cos^2\theta\rangle$ and $\langle\cos^4\theta\rangle$), and the angle β between absorption and emission moments can be determined by experimentally measuring the parallel and perpendicular polarized components of the fluorescence at $\Psi = 0°$ and $\Psi = 90°$. From $\langle\cos^2\theta\rangle$ and $\langle\cos^4\theta\rangle$ the order parameters $\langle P_2\rangle$ and $\langle P_4\rangle$ can be calculated. These are defined as

$$\langle P_2\rangle = \tfrac{1}{2}(3\langle\cos^2\theta\rangle - 1) \tag{8a}$$

$$\langle P_4\rangle = \tfrac{1}{8}(35\langle\cos^4\theta\rangle - 30\langle\cos^2\theta\rangle + 3) \tag{8b}$$

To obtain an approximation of $N(\theta)$ we use the maximum-entropy method, as explained in a previous paper (Bos and Kleijn, 1995a). In this approach no a priori assumptions are made concerning the shape of the distribution function (except that it is continuous). The underlying idea is that the most probable distribution function is the one that can be realized in the greatest number of distinct ways, subject to the known constraints (Bevensee, 1983). The result of such an analysis is a Maxwell-Boltzmann distribution with ordering energy $U(\theta)$ (Van Langen et al., 1989):

$$\begin{aligned} N(\theta) &= \exp(-U(\theta)/kT) \\ &= N_0 \exp\{\lambda_2 P_2(\cos\theta) + \lambda_4 P_4(\cos\theta)\} \end{aligned} \tag{9}$$

N_0 is the normalization factor. A uniquely defined combination of λ_2 and λ_4 can be obtained by fitting the experimentally accessible values $\langle P_2\rangle$ and $\langle P_4\rangle$ using a least-squares method.

MATERIALS AND METHODS

1,2-Dihexadecanoyl-sn-glycero-3-phosphocholine (DPPC) was purchased from Fluka. 2-(3-(Diphenylhexatrienyl)propanoyl)-1-hexadecanoyl-sn-glycero-3-phosphocholine (DPHpPC) and 1-(4-trimethylammoniumphenyl)-6-phenyl-1,3,5-hexatriene, *p*-toluenesulfonate (TMA-DPH) were obtained from Molecular Probes (Eugene, OR). All chemicals were used without further treatment.

A home-built Langmuir trough (area 600 cm^2), equipped with a microbalance for surface pressure measurement by the Wilhelmy-plate method, was used for monolayer transfer. Mixtures of DPPC and DPHpPC (molar ratio 20:1) dissolved in chloroform, or DPPC and TMA-DPH (molar ratio 10:1) dissolved in chloroform/methanol (volume ratio 1:1) were spread on a subphase of pure water ("nanopure," resistivity 18.3 MΩ, pH ~6). After solvent evaporation the monolayer was compressed at a rate of 80 mm^2/s (~1.5×10^{-3} nm^2/s per molecule) to a prespecified surface pressure. Subsequently, the monolayer was allowed to relax for ~60 min. Usually equilibrium was attained (i.e., no detectable change in surface pressure over a time period of 15 min) between 30 and 60 min after compression.

Transfer to a quartz substrate (50 × 20 × 1 mm, Suprasil 2; Heraeus GmbH, Hanau, Germany) was performed by lifting the substrate vertically out of the subphase at a speed of 0.8 mm^2/s. Before transfer the quartz plates were cleaned by overnight immersion in a chromic acid solution, followed by immersion in an alcoholic base solution for a few hours, and then rinsed with water before use. DPPC/DPHpPC monolayers were transferred at two different surface pressures, 30 and 6.5 mN/m, respectively, whereas DPPC/TMA-DPH was transferred only at 30 mN/m. All of the film transfers were performed at a temperature of 21 ± 1°C, and in all cases the transfer ratios were larger than 95%. TIRF and fluorescence microscopy measurements confirmed incorporation of the probe molecules in the supported monolayers, although their final concentration is not known (TMA-DPH, for example, is slightly soluble in water; Huang and Haugland, 1991). Fluorescence microscopy images gave no indication of clustering or phase separation of the probes.

The molecular structure of DPPC monolayers transferred on quartz at various surface pressures has previously been investigated by atomic force microscopy (AFM) (Zhai and Kleijn, 1997). AFM measurements were carried out using a NanoScope III system (Digital Instruments, Santa Barbara, CA), in the contact mode at room temperature in air. Molecular scale images were captured at minimal force, i.e., in the attractive part of the force-distance curve. Therefore, the tip is not pushed into the monolayer, but stays on the surface as a result of adhesion forces. To further minimize artefacts resulting from scanner drift and sample deformation, the height profiles captured in the trace and retrace directions were compared, and scanning was repeated in various directions. Typical AFM images obtained for monolayers transferred at 30 mN/m and 6.5 mN/m are shown in Fig. 3. It was found that incorporation of 5 mol% DPHpPC in the 30 mN/m monolayers does not affect the molecular organization of these layers.

A detailed description of the TIRF set-up has been given before (Bos and Kleijn, 1995b). Here only modifications made for the measurements described in this paper are mentioned. A sealed head pulsed nitrogen laser (model VSL-337ND; Laser Science, Cambridge, MA) with an emission wavelength of 337 nm was utilized for excitation. A horizontally polarized beam was selected using a Glan-Laser polarizing prism (Melles Griot, Zevenaar, The Netherlands). Subsequently, the polarization angle Ψ was adjusted by passage of the beam through a Berek polarization compensator (model 5540; New Focus, Mountain View, CA). In the TIRF cell (filled with water) the quartz substrate with phospholipid monolayer was optically coupled to a quartz prism using immersion liquid. The reflection spot at the solid/liquid interface was approximately 1 mm^2. For orientation measurements detection of the fluorescence took place at a wavelength of 478 nm. In the wavelength range from 400 to 500 nm the detection efficiency of the spectrograph (model 1233; EG&G Princeton Applied Research, Princeton, NJ) is a factor 1.10 better for vertically polarized light than for horizontally polarized light. (Horizontal polarization corresponds to the direction parallel to the plane of incidence.)

All TIRF measurements were carried out at ambient room temperature. Before each series of measurements of $F_{\parallel}(0°)$, $F_{\parallel}(90°)$, $F_{\perp}(0°)$, and $F_{\perp}(90°)$ on a particular monolayer, a controlled background experiment was performed to exclude contributions to the fluorescence by parts of the TIRF cell excited by scattered radiation. Using a bare quartz substrate under experimental conditions that were otherwise the same, both the horizontally and vertically polarized components of the fluorescence were determined for $\Psi = 0°$ and $\Psi = 90°$. Before further data analysis these background values were subtracted from the corresponding values of $F_{\parallel}(0°)$, $F_{\parallel}(90°)$, $F_{\perp}(0°)$, and $F_{\perp}(90°)$.

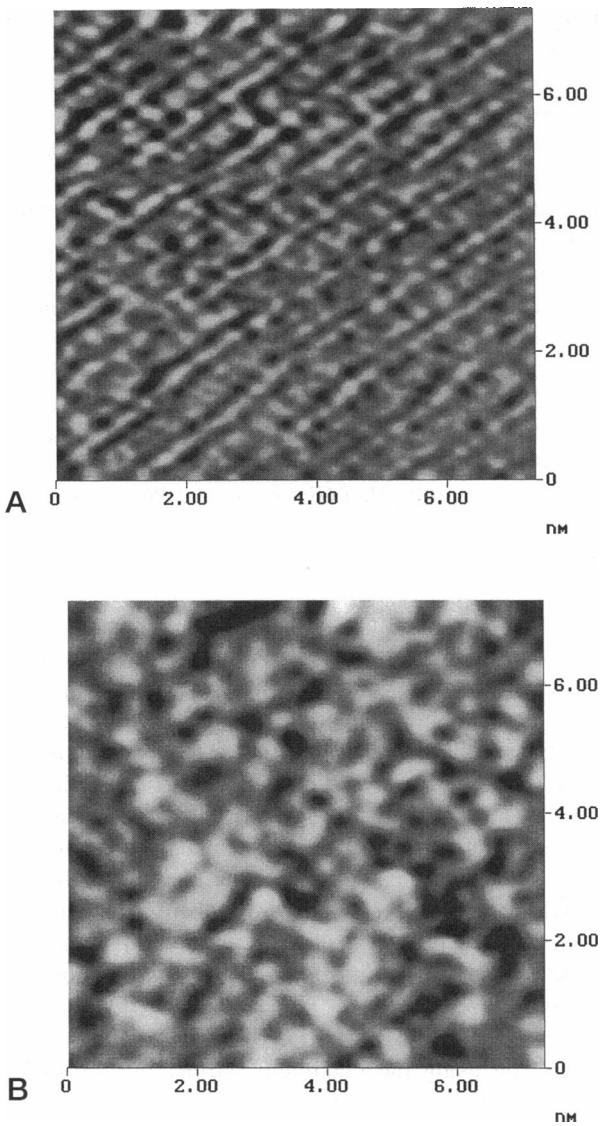

FIGURE 3 AFM images of DPPC monolayers on quartz, transferred at 30 mN/m (*a*) and 6.5 mN/m (*b*). The bright spots in image (a) correspond to the methyl ends of the phospholipid chains (Zhai and Kleijn, 1997).

For analysis of the data in terms of order parameters of the DPH probes, for the components of the evanescent field ϵ_x, ϵ_y, and ϵ_z values of 0.4787, 0.9873, and 1.014 were used, respectively. These values were obtained using the equations given by Harrick (1967), with a refractive index of 1.577 for quartz in the UV region, 1.333 for water, and an angle of incidence of 70°. The dichroic factor γ was taken as 0.98, corresponding to the aperture angle of the detection system (10°) (Burghardt and Thompson, 1984). For a variety of values for β, the constant C and parameters $\langle\cos^2\theta\rangle$ and $\langle\cos^4\theta\rangle$ were calculated according to Eq. 5 using a least-squares numerical fit. Subsequently, for β the value was taken that yielded realistic values for $\langle P_2\rangle$ and $\langle P_4\rangle$, i.e., both located within their physical boundaries, which follow from their definition given in Eq. 8.

RESULTS AND DISCUSSION

For each of the three types of monolayers (i.e., DPPC/DPHpPC transferred at 30 mN/m, DPPC/DPHpPC transferred at 6.5 mN/m, and DPPC/TMA-DPH transferred at 30 mN/m), a number of orientation measurements have been performed. The results in terms of order parameters are depicted in Fig. 4. Before discussing these results in detail, it should be noted that the TIRF measurements show that the various monolayers stay stably on the quartz substrates when brought into contact with water: the observed fluorescence signals are not from the aqueous bulk phase, because the fluorescent probes are not (DPHpPC) or hardly (TMA-DPH) water soluble, whereas TMA-DPH is not fluorescent in aqueous solution (Lentz, 1989). It was found that the total fluorescence intensity is practically the same at every position on the surface.

One might ask how it is possible that a monolayer with hydrophobic tails facing away from the substrate is stable in water. Bringing such a monolayer into contact with water results in unfavorable interactions between the lipid tails and water (for a compact monolayer restricted to interactions between the methyl ends of the tails and water). However, the substrate surface is hydrophilic, i.e., not particularly attractive for the hydrophobic tails either. From AFM measurements (Zhai and Kleijn, 1997) we concluded that there is some water between the headgroups and the solid support (the surface roughness of the bare quartz is much higher than that of quartz covered with a compact phospholipid monolayer). For DPPC LB bilayers on oxidized silicon, Tamm and McConnell (1985) have drawn the same conclusion from lateral diffusion measurements. In contact with water the quartz surface is negatively charged. Although DPPC bears no net charge, there is a net electro-

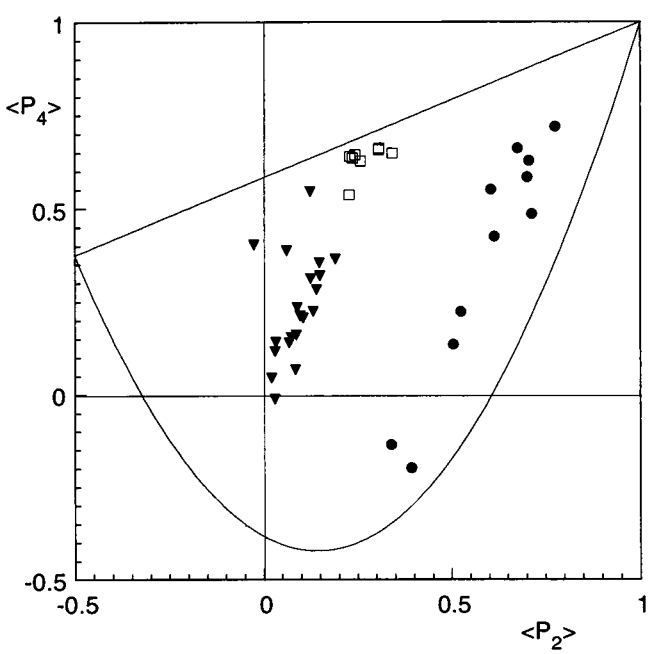

FIGURE 4 Combinations of order parameters $\langle P_2\rangle$ and $\langle P_4\rangle$ obtained for monolayers of DPPC/DPHpPC transferred to quartz at 30 mN/m (●), DPPC/DPHpPC transferred at 6.5 mN/m (▼), and DPPC/TMA-DPH transferred at 30 mN/m (□). The solid curves indicate the physical boundaries of $\langle P_2\rangle$ and $\langle P_4\rangle$.

static attraction between the surface and the lipid headgroups (Tamm and McConnel, 1985).

As can be seen from Fig. 4, there is quite a lot of scatter in the obtained order parameters for each type of monolayer, especially in the case of DPHpPC as the probe molecule. This scatter results mainly from two factors. In the first place, part of the scatter is due to stochastic errors in the orientation measurements. This is illustrated by the fact that generally the spread in $\langle P_4 \rangle$ is larger than in $\langle P_2 \rangle$. The order parameters are calculated from the experimentally accessible parameters $\langle \cos^2\theta \rangle$ and $\langle \cos^4\theta \rangle$, and from Eq. 8 it is easy to see that any experimental errors in these quantities give rise to larger errors in $\langle P_4 \rangle$ than in $\langle P_2 \rangle$. Secondly, the data points in Fig. 4 per monolayer type are results of measurements on various freshly prepared LB films and at different spots. It is quite conceivable that the structural organization varies from film to film and from spot to spot. A similar observation, albeit on a smaller length scale, has been made in AFM measurements: although the DPPC monolayers transferred at 30 mN/m have a regular, compact structure (see Fig. 3 *a*), corresponding to a distorted hexagonal lattice, the exact lattice parameters show local variations. This probably results from variations in substrate topology and discontinuities in the transfer process.

Despite the scatter in the results, there is no overlap in the regions in which the combinations of $\langle P_2 \rangle$ and $\langle P_4 \rangle$ are found for the different monolayers. In Table 1 the averages of the obtained values for $\langle P_2 \rangle$ and $\langle P_4 \rangle$ per monolayer type are listed, together with the corresponding parameters for the orientation distributions as calculated following the maximum-entropy method.

For the DPPC/DPHpPC monolayers transferred at a surface pressure of 30 mN/m, all of the experimental data yielded $\langle P_2 \rangle$ and $\langle P_4 \rangle$ combinations within their physical boundaries, provided that β was taken between 0° and 1°. Apparently, under these conditions the absorption and emission dipole moments of the DPH probe are colinear. For the DPPC/DPHpPC monolayers transferred at a lower pressure of 6.5 mN/m, it was found that physical meaningful combinations of $\langle P_2 \rangle$ and $\langle P_4 \rangle$ were obtained for $\beta = 36 \pm 4°$. Finally, for the DPPC/TMA-DPH monolayers for β, a value of $32 \pm 3°$ was found.

In the literature a variety of values have been reported for the angle between the absorption and emission dipole moments of DPH probes, obtained from fluorescence depolarization experiments. As already mentioned in the Theory section, it has been established that β is sensitive to the environment of the probe molecule. For DPHpPC in multilamellar dispersions of dioleoylphosphatidylethanolamine (DOPE), Cheng (1989) found a β of 29°, whereas Muller et al. (1994a) reported values between 12° and 25° for this probe in small unilamellar vesicles of various lipids. For TMA-DPH in multibilayer lipid systems, Van Ginkel et al. (1986) and Deinum et al. (1988) found values for β in the range of 12–20°; for this probe in vesicles of various lipids Bernsdorff et al. (1995) and Muller et al. (1994b) obtained values between 0° and 19°. For the parent probe DPH, it has been found that β increases with bilayer water content (Van Ginkel et al., 1986; Van Langen et al., 1987) and is lowered by the presence of cholesterol (Kooyman et al., 1983; Van Ginkel et al., 1986; Deinum et al., 1988). For DPH the range of values reported for β (0–35°) is somewhat larger than those for DPHpPC and TMA-DPH (Kooyman et al., 1983; Mulders et al., 1986; Van Ginkel et al., 1986; Muller et al., 1996).

For the interpretation of our TIRF orientation measurements in terms of order parameters, β was initially considered a free variable and then determined, so that the obtained $\langle P_2 \rangle$ and $\langle P_2 \rangle$ were within their physical meaningful parameter space. The small spread in the obtained β values for each type of monolayer strengthens our confidence in this analysis. (However, this small spread does not imply that the assumption of a constant β for all of the DPH probes in a particular monolayer is correct; we will come back to this later.) Furthermore, the values for β found here (0–36°) are in reasonable agreement with previous findings. It should be noted that no literature data are available for the angle between the absorption and emission dipole moments of DPH probes in phospholipid monolayers on solid supports.

Fig. 5 *a* shows the orientation distribution functions $N(\theta)$ obtained by using the maximum-entropy method and the average order parameters listed in Table 1. Fig. 5 *b* gives the corresponding number density functions, defined as $N(\theta) \sin \theta$.

The number density curve for the DPPC/DPHpPC monolayers transferred at 30 mN/m, i.e., from the liquid-condensed (LC) state at the air/water interface, shows that the orientation of the long molecular axis of the DPH groups exhibits a broad distribution around 14° with respect to the normal of the substrate surface; most DPH groups have a tilt angle in the range 5–25°. The DPH containing tail of DPHpPC is assumed to be aligned with the hydrocarbon tails in the DPPC monolayer. Thus the probe order parameters would reflect the overall molecular order in the phospholipid tail region. This assumption seems to be reason-

TABLE 1 Average order parameters, angle between absorption and emission dipole moments of the DPH group, and coefficients of the orientation distribution function as obtained by the maximum-entropy method, for the various monolayers studied

Monolayer type	$\langle P_2 \rangle$	$\langle P_4 \rangle$	β	λ_2	λ_4	N_0
DPPC/DPHpPC, 30 mN/m	0.60	0.37	0°	2.02	1.42	0.219
DPPC/DPHpPC, 6.5 mN/m	0.09	0.25	36°	−1.67	1.78	0.321
DPPC/TMA-DPH, 30 mN/m	0.27	0.63	32°	−4.15	14.3	1.25×10^{-3}

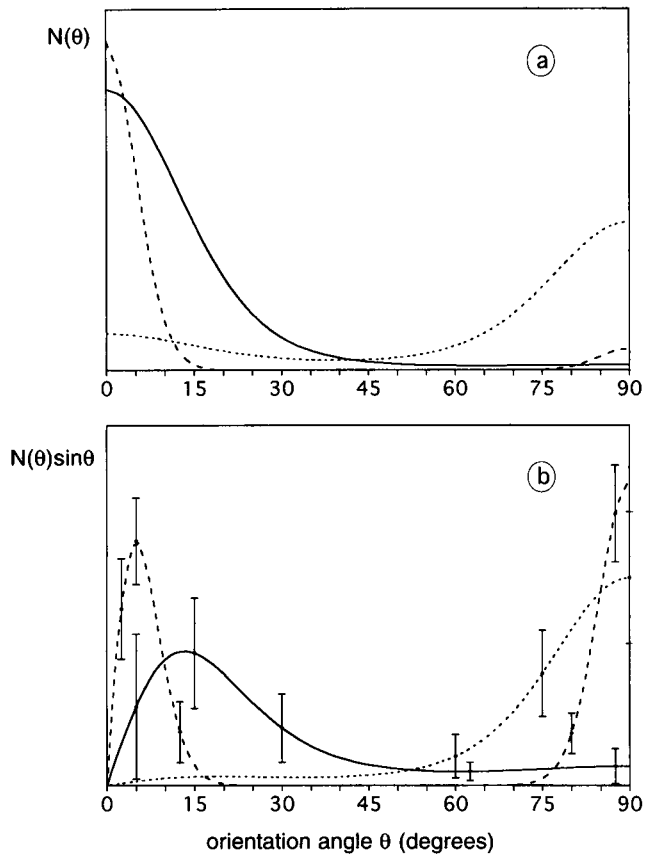

FIGURE 5 (*a*) Orientation distributions $N(\theta)$ as calculated from the average order parameters in Table 1 according to the maximum-entropy method for monolayers of DPPC/DPHpPC transferred to quartz at 30 mN/m (——), DPPC/DPHpPC transferred at 6.5 mN/m (····), and DPPC/TMA-DPH transferred at 30 mN/m (– – –). (*b*) Corresponding number density functions, $N(\theta)$ sin θ; the error bars are based on the standard deviations in the various $N(\theta)$ sin θ curves calculated separately from each of the $\langle P_2 \rangle$, $\langle P_4 \rangle$ combinations given in Fig. 4.

able, because the presence of DPHpPC does not significantly affect the molecular organization of the compact monolayer as observed by AFM (Zhai and Kleijn, 1997). The question of perturbation of phospholipid bilayers by DPHpPC has been addressed in a review by Lentz (1989). Calorimetric measurements on DPPC vesicles have shown that the presence of DPHpPC lowers the phase transition temperature only slightly, demonstrating that the probe does not substantially perturb the overall phase structure of the bilayer membrane. On the other hand, results from differential scanning calorimetry experiments have suggested that DPHpPC disrupts bilayer order in its vicinity.

Because we report here for the first time on the order in single monolayers of phospholipids on solid substrates, comparison with previously published data is not straightforward. In the literature various DPPC tilt angles for different systems, obtained with different techniques, have been reported. For thin DPPC LB films (nine monolayers) transferred at 30 mN/m, Okamura et al. (1991) evaluated an orientation angle of 18° with respect to the substrate normal using infrared reflection-absorption spectroscopy (IRRAS). Hasegawa et al. (1996) determined a tilt angle of 17° in a 10-monolayer DPPC LB film transferred at 40 mN/m, using UV absorption spectroscopy and chlorprozamine as the UV probe. Although these tilt angles seem to be in fair agreement with our results, the problem is that they are obtained from one order parameter only, i.e., from $\langle P_2 \rangle$. A given value for $\langle P_2 \rangle$ can correspond to different orientation distributions, and is in fact insufficient to determine a collective tilt angle (Kooyman et al., 1983; Lafrance et al., 1995). When a tilt angle is calculated from the average $\langle P_2 \rangle$ obtained here (0.60), a value of 31° is obtained; $\langle P_2 \rangle$ values for the above-mentioned systems studied by Okamura et al. and Hasegawa et al. were found in the range 0.8–0.9. The discrepancy between these and our $\langle P_2 \rangle$ value might be explained by the fact that in a single monolayer the influence of the substrate on the ordering is of course much greater than in multilayer LB films.

From IR spectroscopy studies it has been concluded that the conformational and orientational order in the LC phase of a phospholipid monolayer at the air/water interface can be compared with the gel phase of phospholipid bulk systems (Mitchell and Dluhy, 1988). In both cases the conformation of the hydrocarbon tails is mostly all-*trans*. For DPPC in the gel phase, IR attenuated total reflection (IR-ATR) experiments revealed $\langle P_2 \rangle$ values between 0.7 and 0.8 (Okamura et al., 1990, 1991).

Synchrotron x-ray diffraction on DPPC monolayers in the LC phase at the air-water interface revealed preferential tilt angles of 25–30°, depending on surface pressure (Brezesinski et al., 1995; Möhwald et al., 1995). X-ray diffraction experiments yield directly the orientation without relying on order parameters. These relatively high tilt angles are contributed to hydration of the phosphatidylcholine headgroup, resulting in a bulky head that does not allow for a projected area on the air/water interface below 0.22–0.23 nm^2 per tail. However, for DPPC monolayers on quartz transferred at 30 mN/m, our AFM measurements revealed an average area of 0.20 nm^2 per hydrocarbon chain, corroborating the lower preferential tilt angles found here. For oriented stacks of bilayers, deposited by pipetting solutions of phospholipids on a substrate, x-ray diffraction revealed orientation angles of 20–35°, depending on the degree of hydration of the films (Blaurock and McIntosh, 1986; Katsaras et al., 1992, 1995; Tristam-Nagle et al., 1993).

Determination of the orientational order by fluorescence depolarization experiments using DPH-based probes has been performed only on bulk systems, i.e., multibilayer and vesicle systems. For phosphatidylcholines, preferential tilt angles of 10–30° with respect to the bilayer normal have been obtained (Kooyman et al., 1983; Van Langen et al., 1989; Florine-Casteel, 1990). In some cases (Mulders et al., 1986; Deinum et al., 1988) for phosphatidylcholine multibilayers in the gel phase practically the same combinations of $\langle P_2 \rangle$ and $\langle P_4 \rangle$ values have been found as obtained here for DPPC monolayers transferred from the LC phase.

At a surface pressure of 6.5 mN/m a DPPC monolayer at the air-water interface is in the liquid-expanded (LE) phase. AFM images of such monolayers transferred to quartz show a loosely packed, irregular structure (Fig. 3 *b*). The combination of order parameters for such layers obtained here is for some of the investigated locations on the LB films very near that for a random distribution ($\langle P_2 \rangle = \langle P_4 \rangle = 0$; see Fig. 4). From Fig. 5 *b* it can be seen that—averaged over various films and spots—most of the DPH groups are at an angle of 70° or more with respect to the normal of the substrate surface (i.e., lying more or less flat on the surface), whereas only a small part of the DPH-containing phospholipid tails is standing up. IRRAS measurements (Mitchell and Dluhy, 1988) have shown that DPPC monolayers at the air/water interface in the LE phase have a highly disordered conformation of the hydrocarbon chains, with a large number of *gauche* conformers. Therefore, it does not seem appropriate to speak in terms of tilt angles of the lipid chains, and the low values of the order parameters merely reflect the disorder in the system.

For TMA-DPH in DPPC monolayers transferred at 30 mN/m, a bimodal distribution is clearly found. In this case about half of the TMA-DPH molecules have their long molecular axes normal to the substrate surface (modal tilt angle is ~5°), and the other half are lying more or less flat on the surface (see Fig. 5 *b*). We suspect that this latter population is localized between the headgroups of the phospholipids and the negatively charged substrate surface (TMA-DPH itself is positively charged). Bimodal distributions have also been reported for TMA-DPH in lipid bilayer systems. In a fluorescence polarization microscopy study on DPPC vesicles, Florine-Casteel (1990) has found that in the gel phase about 5% of the TMA-DPH molecules are parallel to the bilayer surface, whereas the rest of the probe molecules exhibit an orientation angle around 30° with respect to the bilayer normal. Neutron scattering experiments of Pebay-Peyroula et al. (1994) revealed that in oriented multilayers of gel-phase DPPC on glass no less than 40% of the TMA-DPH molecules are located close and parallel to the bilayer surface, whereas the rest were found to be at angles around 25° relative to the bilayer normal.

As for the part of the TMA-DPH molecules exhibiting orientation angles around 5°, these are expected to reflect the order near the glycerol-acyl chain linkage of the phospholipids (Parente and Lentz, 1985; Lentz, 1989). Apart from having a smaller tilt angle, their orientation distribution is much narrower than that of the DPHpPC probes in similar monolayers (Fig. 5 *b*). This points to a stronger ordering near the headgroup region than further away from the substrate surface. IRRAS measurements on DPPC monolayers at the air/water interface have shown comparable results, i.e., the chains exhibit more conformational order adjacent to the interface than at their tails (Gericke et al., 1996)

Comparing the sets of data points for the different monolayers in Fig. 4, it is striking that the scatter in the results for the DPPC/DPHpPC monolayers transferred at 30 mN/m is much larger than for the DPPC/TMA-DPH monolayers transferred at the same surface pressure. Apparently, variation in the ordering of the TMA-DPH molecules from film to film and from spot to spot is much less than that of the DPHpPC molecules. This is another indication that ordering near the headgroup region is stronger and better defined than in the outer tail region of the DPPC monolayer.

With respect to the assumption that the angle β between absorption and emission dipole moment is constant, we expect it to be justified for the DPHpPC molecules in the monolayers transferred at 30 mN/m. These layers have a very compact, regular structure, and the DPH groups are all embedded in the tail region of the monolayer. For the monolayers transferred at 6.5 mN/m, the structure as observed by AFM is much more open and almost random. This implies that the environment of the individual DPH probes varies and that there is some distribution in β. Furthermore, for the DPPC/TMA-DPH monolayers transferred at 30 mN/m, the assumption of a constant β appears to be less applicable. Because the TMA-DPH molecules can be divided into two populations (molecules that are lying flat, probably between substrate surface and phospholipid headgroups, and molecules that are aligned between the DPPC molecules), there probably is also a bimodal distribution in β. Provided that β is not directly correlated to the molecular tilt angle, this has no consequences for our analysis. However, it would be more appropriate to give values for $\langle \cos^2\beta \rangle$ than for β: from Eq. 5 it follows that this is in fact the experimentally obtainable quantity.

CONCLUSIONS

Using TIRF and two kinds of DPH-based probes, DPHpPC and TMA-DPH, we have determined the second- and fourth-rank orientational order parameters of DPPC Langmuir-Blodgett monolayers on quartz. Furthermore, the angle between the absorption and emission dipole moments of the probes has been evaluated. For monolayers transferred from the liquid-condensed phase, tilt angles were broadly distributed around 14° in the lipid tail region and more sharply distributed around 5° near the glycerol-acyl chain linkage. It was found that a large fraction of the TMA-DPH probe molecules are oriented more or less parallel to the monolayer, probably between the phospholipid headgroups and the substrate surface. Monolayers transferred from the liquid-expanded phase show a more random distribution. All of the results are—as far as comparison can be made—in reasonable agreement with previously published data and show that TIRF combined with maximum-entropy analysis is a good instrument for determining the order and preferential orientation in very thin phospholipid layers (monolayers, bilayers, . . .) on solid substrates.

REFERENCES

Axelrod, D. 1979. Carbocyanine dye orientation in red cell membrane studied by microscopic fluorescence polarisation. *Biophys. J.* 26: 557–573.

Bernsdorff, C., R. Winter, T. L. Hazlett, and E. Gratton. 1995. Influence of cholesterol and β-sitosterol on the dynamic behaviour of DPPC as detected by TMA-DPH and PyrPC fluorescence: a fluorescence lifetime distribution and time-resolved anisotropy study. *Ber. Bunsen-ges. Phys. Chem.* 99:1479–1488.

Bevensee, R. M. 1983. Maximum Entropy Solutions to Scientific Problems. Prentice Hall, Englewood Cliffs, NJ.

Blaurock, A. E., and T. J. McIntosh. 1986. Structure of the crystalline bilayer in the subgel phase of dipalmitoylphosphatidylglycerol. *Biochemistry.* 25:299–305.

Bos, M. A., and J. M. Kleijn. 1995a. Determination of the orientation distribution of adsorbed fluorophores using TIRF. I. Theory. *Biophys. J.* 68:2566–2572.

Bos, M. A., and J. M. Kleijn. 1995b. Determination of the orientation distribution of adsorbed fluorophores using TIRF. II. Measurements on porphyrin and cytochrome c. *Biophys. J.* 68:2573–2579.

Brezesinski, G., A. Dietrich, B. Struth, C. Böhm, W. G. Bouwman, K. Kjaer, and H. Möhwald. 1995. Influence of ether linkages on the structure of double-chain phospholipid monolayers. *Chem. Phys. Lipids.* 76:145–157.

Burghardt, T. P., and N. L. Thompson. 1984. Effect of planar dielectric interfaces on fluorescence emission and detection. Evanescent excitation with high-aperture collection. *Biophys. J.* 46:729–737.

Cheng, K. H. 1989. Fluorescence depolarization study of lamellar liquid crystalline to inverted cylindrical micellar phase transition of phosphatidylethanolamine. *Biophys. J.* 55:1025–1031.

Clerc, S. G., and T. E. Thompson. 1995. Permeability of dimyristoyl phosphatidylcholine/dipalmitoyl phosphatidylcholine bilayer membranes with coexisting gel and liquid-crystalline phases. *Biophys. J.* 68:2333–2341.

Deinum, G., H. van Langen, G. van Ginkel, and Y. K. Levine. 1988. Molecular order and dynamics in planar lipid bilayers: effects of unsaturation and sterols. *Biochemistry.* 27:852–860.

Florine-Casteel, K. 1990. Phospholipid order in gel- and fluid-phase cell-size liposomes measured by digitized video fluorescence polarization microscopy. *Biophys. J.* 57:1199–1215.

Gericke, A., D. J. Moore, R. K. Erukulla, R. Bittman, and R. Mendelsohn. 1996. Partially deuterated phospholipids as IR structure probes of conformational order in bulk and monolayer phase. *J. Mol. Struct.* 379: 227–239.

Harrick, N. J. 1967. Internal Reflection Spectroscopy. John Wiley/ Interscience, New York.

Hasegawa, T., Y. Ushiroda, M. Kawaguchi, Y. Kitazawa, M. Nishiyama, A. Hiraoka, and J. Nishijo. 1996. UV absorption spectroscopic analysis of the molecular orientation of a drug penetrated into a DPPC membrane. *Langmuir.* 12:1566–1571.

Hasmonay, H., A. Hochapfel, C. Betrencourt, A. Tahir, and P. Peretti. 1994. Lasalocid and biomimetic membranes: insertion in Langmuir films of lipids. *Biochim. Biophys. Acta.* 1193:287–292.

Huang, Z., and R. P. Haugland. 1991. Partition coefficients of fluorescent probes with phospholipid membranes. *Biochem. Biophys. Res. Commun.* 181:166–171.

Hui, S. W., D. F. Parsons, and M. Cowden. 1974. Electron diffraction of wet phospholipid bilayers. *Proc. Natl. Acad. Sci. USA.* 71:5068–5072.

Katsaras, J., V. A. Raghunathan, E. J. Dufourc, and J. Dufourcq. 1995. Evidence for a two-dimensional molecular lattice in subgel phase DPPC bilayers. *Biochemistry.* 34:4684–4688.

Katsaras, J., D. S. C. Yang, and R. M. Epand. 1992. Fatty-acid chain tilt angles and directions in dipalmitoyl phosphatidylcholine bilayers. *Biophys. J.* 63:1170–1175.

Kooyman, R. P. H., M. H. Vos, and Y. K. Levine. 1983. Determination of orientational order parameters in oriented lipid membrane systems by angle-resolved fluorescence depolarization experiments. *Chem. Phys.* 81:461–472.

Lafrance, C. P., A. Nabet, R. E. Prud'homme, and M. Pézolet. 1995. On the relationship between the order parameter $\langle P_2(\cos\theta)\rangle$ and the shape of orientation distribution. *Can. J. Chem.* 73:1497–1505.

Leermakers, F. A. M., and A. Nelson. 1990. Substrate-induced structural changes in electrode-adsorbed lipid layers: a self-consistent field theory. *J. Electroanal. Chem.* 278:53–72.

Lentz, B. R. 1989. Membrane "fluidity" as detected by diphenylhexatriene probes. *Chem. Phys. Lipids.* 50:171–190.

Mitchell, M. L., and R. A. Dluhy. 1988. In situ FT-IR investigation of phospholipid monolayer phase transitions at the air-water interface. *J. Am. Chem. Soc.* 110:712–718.

Möhwald, H., H. Baltes, M. Schwendler, C. A. Helm, G. Brezesinski, and H. Haas. Phospholipid and protein monolayers. 1995. *Jpn. J. Appl. Phys.* 34:3906–3913.

Mulders, F., H. van Langen, G. van Ginkel, and Y. K. Levine. 1986. The static and dynamic behaviour of fluorescent probe molecules in lipid bilayers. *Biochim. Biophys. Acta.* 859:209–218.

Muller, J. M., E. E. van Faassen, and G. van Ginkel. 1994a. The interpretation of the time-resolved fluorescence anisotropy of diphenylhexatriene-phosphatidylcholine using the compound motion model. *Biochem. Biophys. Res. Commun.* 201:709–715.

Muller, J. M., E. E. van Faassen, and G. van Ginkel. 1994b. Experimental support for a novel compound motion model for the time-resolved fluorescence anisotropy decay of TMA-DPH in lipid vesicle bilayers. *Chem. Phys.* 185:393–404.

Muller, J. M., G. van Ginkel, and E. E. van Faassen. 1996. Effect of lipid molecular structure and gramicidin A on the core of lipid vesicle bilayers. A time-resolved fluorescence depolarization study. *Biochemistry.* 35:488–497.

Nelson, A., and H. P. van Leeuwen. 1989. Metal voltammetry at dioleoyl lecithin (di-O-PC) coated mercury electrodes: Cd, Cu, Eu, Pb, V and Zn and the effect of electrolyte composition. *J. Electroanal. Chem.* 273: 183–199.

Nikolelis, D. P., C. G. Siontorou, V. G. Andreou, K. G. Viras, and U. J. Krull. 1995. Bilayer lipid membranes as electrochemical detectors for flow injection immunoanalysis. *Electroanalysis.* 7:1082–1089.

Okamura, E., J. Umemura, and T. Takenaka. 1990. Orientation studies of hydrated dipalmitoylphosphatidylcholine multibilayers by polarized FTIR-ATR spectroscopy. *Biochim. Biophys. Acta.* 1025:94–98.

Okamura, E., J. Umemura, and T. Takenaka. 1991. Fourier transform infrared/attenuated total reflection study on subtransition of hydrated dipalmitoylphosphatidylcholine multibilayers. *Vib. Spectrosc.* 2:95–100.

Parente, R. A., and B. R. Lentz. 1985. Advantages and limitations of 1-palmitoyl-2-[[2-[4-(6-phenyl-trans-1, 3, 5-hexatrieny)phenyl]ethyl] carbonyl]-3-sn-phosphatidylcholine as a fluorescent membrane probe. *Biochemistry.* 24:6178–6185.

Pebay-Peyroula, E., E. J. Dufourc, and A. G. Szabo. 1994. Location of diphenyl-hexatriene and trimethylammonium-diphenyl-hexatriene in dipalmitoylphosphatidylcholine bilayers by neutron diffraction. *Biophys. Chem.* 53:45–56.

Sharma, A., and K. R. Rogers. 1994. Biosensors. *Meas. Sci. .Technol.* 5:461–472.

Shinitzky, M., and Y. Barenholz. 1974. Dynamics of the hydrocarbon layer in liposomes of lecithin and sphingomyelin containing dicetylphosphate. *J. Biol. Chem.* 249:2652–2657.

Tamm, L. K., and H. M. McConnell. 1985. Supported phospholipid bilayers. *Biophys. J.* 47:105–113.

Thompson, N. L., and T. P. Burghardt. 1986. Total internal reflection fluorescence measurement of spatial and orientational distributions of fluorophores near planar dielectric interfaces. *Biophys. Chem.* 25:91–97.

Tristam-Nagle, S., R. Zhang, R. M. Suter, C. R. Worthington, W. J. Sun, and J. F. Nagle. 1993. Measurement of chain tilt angle in fully hydrated bilayers of gel phase lecithins. *Biophys. J.* 64:1097–1109.

Van Ginkel, G., L. J. Korstanje, H. van Langen, and Y. K. Levine. 1986. The correlation between molecular orientational order and reorientational dynamics of probe molecules in lipid multibilayers. *Faraday Discuss. Chem. Soc.* 81:49–61.

Van Langen, H., D. Engelen, G. van Ginkel, and Y. K. Levine. 1987. Headgroup hydration in egg-lecithin multibilayers affects the behaviour of DPH probes. *Chem. Phys. Lett.* 138:99–104.

Van Langen, H., C. A. Schrama, G. van Ginkel, G. Ranke, and Y. K. Levine. 1989. Order and dynamics in the lamellar L_α and in the hexagonal H_{II} phase: dioleoylphosphatidyl-ethanolamine studied with angle-resolved fluorescence depolarization. *Biophys. J.* 55:937–947.

Zhai, X., and J. M. Kleijn. 1997. Molecular structure of dipalmitoylphosphatidylcholine Langmuir–Blodgett monolayers studied by atomic force microscopy. *Thin Solid Films.* In press.